Diabetes Adversely Affects Macrophages During Atherosclerotic Plaque Regression in Mice

Saj Parathath,[1] Lisa Grauer,[1] Li-Shin Huang,[2] Marie Sanson,[1] Emilie Distel,[1] Ira J. Goldberg,[2] and Edward A. Fisher[1,3]

OBJECTIVE—Patients with diabetes have increased cardiovascular risk. Atherosclerosis in these patients is often associated with increased plaque macrophages and dyslipidemia. We hypothesized that diabetic atherosclerosis involves processes that impair favorable effects of lipid reduction on plaque macrophages.

RESEARCH DESIGN AND METHODS—Reversa mice are LDL receptor–deficient mice that develop atherosclerosis. Their elevated plasma LDL levels are lowered after conditional knockout of the gene encoding microsomal triglyceride transfer protein. We examined the morphologic and molecular changes in atherosclerotic plaques in control and streptozotocin-induced diabetic Reversa mice after LDL lowering. Bone marrow–derived macrophages were also used to study changes mediated by hyperglycemia.

RESULTS—Reversa mice were fed a western diet for 16 weeks to develop plaques (baseline). Four weeks after lipid normalization, control (nondiabetic) mice had reduced plasma cholesterol (−77%), plaque cholesterol (−53%), and plaque cells positive for macrophage marker CD68+ (−73%), but increased plaque collagen (+116%) compared with baseline mice. Diabetic mice had similarly reduced plasma cholesterol, but collagen content increased by only 34% compared with baseline; compared with control mice, there were lower reductions in plaque cholesterol (−30%) and CD68+ cells (−41%). Diabetic (vs. control) plaque CD68+ cells also exhibited more oxidant stress and inflammatory gene expression and less polarization toward the anti-inflammatory M2 macrophage state. Many of the findings in vivo were recapitulated by hyperglycemia in mouse bone marrow–derived macrophages.

CONCLUSIONS—Diabetes hindered plaque regression in atherosclerotic mice (based on CD68+ plaque content) and favorable changes in plaque macrophage characteristics after the reduction of elevated plasma LDL. ***Diabetes*** **60:1759–1769, 2011**

Type 1 and 2 diabetic patients have earlier onset and more extensive atherosclerosis than similar aged nondiabetic patients. Moreover, the presence of diabetes is associated with more coronary events and worse clinical outcomes (1,2). This might reflect the presence of plaques that are more vulnerable to rupture. Indeed, careful pathologic assessment of atherosclerotic plaques shows that diabetes is associated with more macrophages and lipid-rich areas (3), features of unstable plaques. Although studies in type 1 diabetes have established that more intensive glucose management reduces cardiovascular events (4), clinical trial data in type 2 diabetes remain controversial. The reasons for this are debated and might reflect differences in pathobiology, therapy, or extent of disease when the trials were initiated.

Current clinical practice to reduce cardiovascular risk in diabetes includes plasma LDL lowering, which should not only retard the progression of atherosclerosis, but also promote its regression. Given the importance of macrophages in plaque development and pathology (5), the effects of plasma lipid changes on these cells have been an active area of research. In our own studies, we have shown in a surgical transplant model that the content of monocyte-derived CD68+ cells (mostly macrophages and macrophage foam cells) in mouse atherosclerotic plaques declined quickly in normolipidemic conditions. Furthermore, some plaque CD68+ cells were shown to emigrate to regional and systemic lymph nodes in a process dependent on the chemokine (C-C) motif receptor-7 (CCR7) (6).

It is now recognized that macrophage phenotypes vary (7). Inflammatory macrophages, often referred to as M1 macrophages, are involved in pathogen recognition and inflammatory cytokine secretion. Tissue repair is thought to be mediated by M2, or alternatively activated, macrophages (8). Both M1 and M2 macrophages, as well as monocyte-derived dendritic cells, are found in human and mouse atherosclerotic plaques (9,10), with the M1 type thought to play a critical role in the progression of atherosclerosis.

In the current report, we have focused on whether the diabetic state negatively influences the ability of plasma lipid reduction to regress atherosclerotic plaques. Given the importance of both the amount and the characteristics of plaque macrophages to the disease process, we examined whether diabetes interfered with a reduction in the content of macrophages or in their inflammatory state after the repression of hyperlipidemia. To accomplish this, we turned to the Reversa mouse, in which the hyperlipidemia of the LDL receptor knockout (*LdLr*$^{-/-}$) mouse can be reduced by the conditional inactivation of the microsomal triglyceride transfer protein gene (*Mttp*) (11). Atherosclerosis was allowed to develop in Reversa mice before they were made diabetic by streptozotocin (STZ) injection to avoid effects of diabetes on plaque progression. Hyperlipidemia then was repressed by *Mttp* ablation in both normoglycemic and diabetic mice. The morphometric and histologic changes in the plaques, as well as the molecular changes in CD68+ cells laser-captured from the plaques, were then determined. Studies of the effects of hyperglycemia on cultured bone marrow–derived macrophages (BMDMs) were performed to extend the results.

From the [1]Department of Medicine and the Leon H. Charney Division of Cardiology/Marc and Ruti Bell Program in Vascular Biology, New York University School of Medicine, New York, New York; the [2]Department of Medicine, Division of Preventive Medicine, Columbia University College of Physicians and Surgeons, New York, New York; and the [3]Department of Cardiovascular Medicine, University of Oxford, Oxford, U.K.
Corresponding author: Edward A. Fisher, edward.fisher@nyumc.org.
Received 2 June 2010 and accepted 7 March 2011.
DOI: 10.2337/db10-0778
This article contains Supplementary Data online at http://diabetes.diabetesjournals.org/lookup/suppl/doi:10.2337/db10-0778/-/DC1.

RESEARCH DESIGN AND METHODS

Animals. Reversa mice ($LdLr^{-/-}Apob^{100/100}Mttp^{fl/fl}Mx1\text{-}Cre^{+/+}$) have been described previously (11). Animals were cared for in accordance with the National Institutes of Health guidelines and the New York University Institutional Animal Care and Use Committee (Protocol 090908). At 4 weeks of age, pups were weaned and placed on a western diet (Catalog no. 100244; Dyets Inc., Bethlehem, PA). After 15 weeks on the diet, some mice were given intraperitoneal injections of citrate buffer or, to mimic type 1 diabetes, low-dose STZ (50 mg/kg; Sigma-Aldrich, St. Louis, MO) (12) according to the protocol of the National Institutes of Health-funded Animal Models of Diabetic Complications Consortium (www.AMDCC.org). After citrate or STZ injections, the group of nontreated mice (baseline group) was killed, and aortic roots and arches were harvested. To reverse the hyperlipidemic lipid profile by conditionally inactivating the *Mttp* gene, both citrate- and STZ-treated mice (regression and regression/STZ groups, respectively) were given intraperitoneal injections of polyinosinic polycytidylic RNA (pIpC) (Sigma-Aldrich) 15 mg/kg every other day for a total of four injections (11). The mice were also switched to a standard chow diet to obtain maximal lipid-lowering effects. All mice were killed 4 weeks after the last injection of pIpC. At the time of tissue harvest, blood was collected via heart puncture for plasma analyses.

Cell culture. BMDMs were prepared from monocytes isolated from the tibia and femur of 6–8-week-old Reversa mice as previously described (13). Typically, cells were incubated for 7 days in Dulbecco's modified Eagle's medium (DMEM), 10% FBS, and 10 ng/mL macrophage colony-stimulating factor (PeproTech, Inc., Rocky Hill, NJ) in normal D-glucose (100 mg/dL) to promote their differentiation into unactivated (M0) macrophages. Cells were then incubated in DMEM containing "normal D+L-glucose" (100 mg/dL D-glucose + 350 mg/dL L-glucose) ± interleukin (IL)-4 (10 ng/mL; PeproTech, Inc.) or high D-glucose (450 mg/dL D-glucose) ± IL-4 (10 ng/mL) in 1% FBS for 24 h. The L-glucose was used to control for changes in osmolarity (see RESULTS for more details). IL-4 was used as a standard polarizer of macrophages to the M2 state (13).

Plasma measurements and lipoprotein analyses. Total cholesterol, free fatty acid, and triglyceride concentrations were measured using colorimetric assays (all kits from Wako Diagnostics, Richmond, VA). The distribution of lipids within the plasma lipoproteins was determined by fractionating the plasma (pooled from five mice per group) using fast protein liquid chromatography followed by a colorimetric assay for total cholesterol (11). For glucose measurements, mice were fasted for 4 h, and glucose in tail blood was measured using a blood glucose monitor (TrueTrack Smart System, Nipro Diagnostics, Inc., Fort Lauderdale, FL). IL-6 and monocyte chemoattractant protein-1 (MCP-1) were measured using an ELISA kit from eBiosciences (San Diego, CA) according to the manufacturer's protocol.

Histochemical analyses of tissues and cells. Aortic roots were harvested from each mouse after perfusion with an RNAse inhibitor (Ambion, Austin, TX), frozen in optimal cutting temperature compound, and serial-sectioned at a thickness of 6 μm onto glass slides. For immunostaining of CD68 (macrophage marker), slides were fixed in 100% acetone and exposed to primary anti-CD68 antiserum (Serotec, Raleigh, NC), followed by biotinylated secondary antibody, with visualization using a kit from Vector Laboratories, Inc. (Burlingame, CA).

Actin was visualized by fluorescein isothiocyanate (FITC)-conjugated anti-β-actin (Abcam, Cambridge, MA) or by FITC-phalloidin (Invitrogen, Carlsbad, CA). Tubulin was detected by antitubulin (Sigma-Aldrich) and visualized by probing with FITC-conjugated anti-rabbit secondary antibody (Jackson ImmunoResearch Laboratories, West Grove, PA). Microscopic images of aortic root sections were digitized, and morphometric measurements were performed using Image Pro Plus software (14).

For collagen quantification, slides were stained with picrosirius red as previously reported (14), and collagen was visualized using polarizing light microscopy (15). Tissue content of neutral lipids (which in plaques mainly consists of cholesteryl ester) and free cholesterol were detected by Oil-Red O (Sigma-Aldrich) and filipin (Sigma-Aldrich) staining, respectively, using sections fixed in 10% formalin and stained as described previously (16,17). Slides were mounted in Vectashield containing DAPI for nuclear staining (Vector Laboratories).

Frozen aortic root sections were stained for oxidative stress using dihydroethidium (Invitrogen) as described previously (18). BMDMs were incubated for 24 h in normal D-glucose (100 mg/dL D-glucose + 350 mg/dL L-glucose) or high D-glucose medium (450 mg/dL D-glucose). The cells were then washed and treated with MitoSOX (Molecular Probes, Eugene, OR) following the manufacturer's protocol. The cells were subjected to the C6 Flow Cytometer (Accuri, Ann Arbor, MI), and cells with MitoSOX staining were observed in the phycoerythrin channel. Another group of cells from the above conditions were plated on chamber slides and counterstained with DAPI. The staining was quantified using Image Pro Plus software.

Laser capture microdissection and quantitative (real-time) PCR. CD68+ cells were selected from atherosclerotic plaques by laser capture microdissection (LCM). All LCM procedures were performed under RNase-free conditions. Aortic root sections were stained with hematoxylin-eosin as previously described (19,20). Foam cells were then identified under a microscope and verified by positive CD68 staining. For each animal, CD68+ cells were captured from 50–60 frozen sections. After LCM, RNA was isolated using the PicoPure Kit (Molecular Devices, Inc., Sunnyvale, CA), and quality and quantity were determined using an Agilent 2100 Bioanalyzer (Agilent Technologies, Santa Clara, CA). RNA was converted to cDNA and amplified using the WT-Ovation Pico RNA Amplification Kit (NuGEN, San Carlos, CA). RT-PCR was performed using a 7300 RT-PCR System (Applied Biosystems, Carlsbad, CA), and data were analyzed using standard curves generated for each set of primers/probe (Supplementary Table 1).

Functional studies in vitro. For arginase activity, we measured urea formation according to the manufacturer's protocol (QuantiChrom, BioAssay Systems, Hayward, CA). In brief, media were collected 24 h after treatment of BMDMs with high D-glucose + IL-4 or normal glucose (100 mg/dL D-glucose + 350 mg/dL L-glucose) + IL-4. Urea levels were measured and adjusted by volume and protein concentration.

Cell spreading. BMDMs were incubated for 24 h in normal D-glucose (100 mg/dL D-glucose + 350 mg/dL L-glucose) or high D-glucose (450 mg/dL) medium. Cells were then replated onto collagen-coated chamber slides (Fisher Scientific, Waltham, MA) and incubated for 2 h in normal or high glucose medium. Cells were stained for actin using FITC-phalloidin, and cell area was quantified using Image Pro Plus software.

Statistical analysis. Data are expressed as the mean ± SEM and were analyzed using the two-tailed Student t test or one-way ANOVA followed by Bonferroni's multiple comparison test. $P < 0.05$ was considered to be significant. All tests were performed using the Prism software (GraphPad Software, Inc., La Jolla, CA).

RESULTS

Plasma cholesterol and lipoprotein levels. The study protocol is diagrammed in Fig. 1*A*. Reversa mice were weaned and then fed a western diet for 16 weeks to allow advanced plaques to develop. Mice were separated into three groups: baseline mice killed at 16 weeks and two regression groups (regression and the diabetic regression/STZ) that were injected with pIpC to conditionally delete the *Mttp* gene to reduce plasma lipid levels (11). The regression/STZ mice were administered an intraperitoneal injection of STZ for 5 days preceding pIpC treatment. This protocol did not increase the glucose or the plasma lipids during the 1-week interval between the STZ and pIpC treatments (data not shown). Before pIpC, total plasma cholesterol (Fig. 1*B*) and fasting glucose levels (Fig. 1*C*) were similar in the mice assigned to the baseline and the two regression groups: Levels of plasma cholesterol averaged ~670 mg/dL and glucose ~125 mg/dL in all groups. Fast protein liquid chromatography analysis of plasma showed the majority of cholesterol to be in the LDL fraction (Fig. 1*D*). Four weeks after pIpC injections, regression and regression/STZ mice had similarly reduced plasma total cholesterol levels (134 ± 6 vs. 133 ± 8 mg/dL) (Fig. 1*B*), without evidence of remnant lipoproteins in the diabetic mice (Fig. 1*D*). Regression/STZ mice had a plasma glucose level fourfold greater than that of regression mice (480 ± 26 vs. 122 ± 7 mg/dL) (Fig. 1*C*). Other lipid parameters, including free fatty acids and triglycerides, were not different between the different groups (Fig. 1*E* and *F*). There was a 16.5% decrease in weight in the regression/STZ group compared with the regression group (Fig. 1*G*).

We also examined general inflammation at the end of the study by measuring IL-6 and MCP-1 in plasma from both regression and regression/STZ mice. Regression/STZ mice have similarly low levels of IL-6 and MCP-1 compared with regression and saline-injected (negative control) groups (Supplementary Fig. 1), whereas lipopolysaccharide-treated

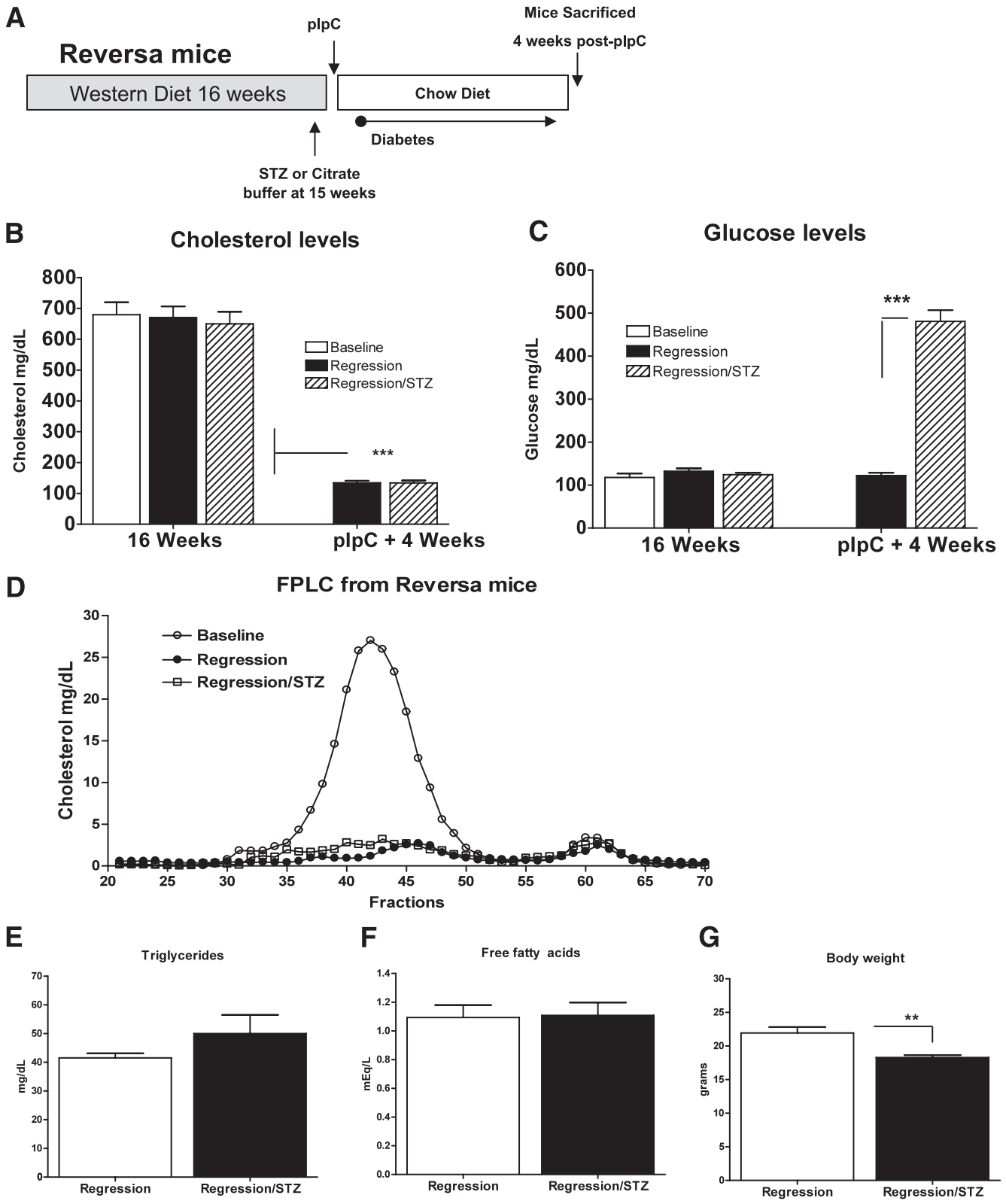

FIG. 1. Experimental design and plasma lipid and glucose data. *A*: Reversa mice were placed on a western diet for 16 weeks. A group of animals (n = 10) was killed at 16 weeks of western diet and used as the baseline group. Two other groups of animals (n = 10 each) received citrate buffer or STZ at 15 weeks. At 16 weeks, regression and regression/STZ groups received pIpC injections and were switched to a chow diet. Animals were killed 4 weeks after the last pIpC injection. Plasma cholesterol (*B*) and glucose levels (*C*) were measured at the 16-week time point and at the end of the experiment. *D*: Plasma samples were also analyzed by fast protein liquid chromatography (FPLC) using pooled plasma from five animals. Total cholesterol was measured in each fraction. Plasma triglycerides (*E*), nonesterified free fatty acids (*F*), and body weight (*G*) were also measured at the end of the experiment. Data (mean ± SEM) were analyzed using one-way ANOVA followed by Bonferroni's multiple comparison test (*B*) or Student two-tailed t test (*C* and *G*). $P < 0.05$ values were considered to be significant, $^{**}P < 0.01$ and $^{***}P < 0.001$.

mice (positive control) showed high plasma levels of both IL-6 and MCP-1.

Changes in plaque area and composition in regression and regression/STZ mice after the reduction of hyperlipidemia. Diabetes significantly impaired the decrease in plaque CD68+ cells after hyperlipidemia was reduced (Fig. 2*A* and *C*). Compared with baseline mice, there was a 73% decrease in plaque CD68+ cells in the regression group. In contrast, in the regression/STZ group, the decrease in plaque CD68+ cells was only 41%.

It is surprising that despite the differences in CD68+ cell content, there was little variation in the absolute area of aortic root plaques in regression (0.46 ± 1 mm^2) and regression/STZ groups (0.42 ± 0.1 mm^2 compared with

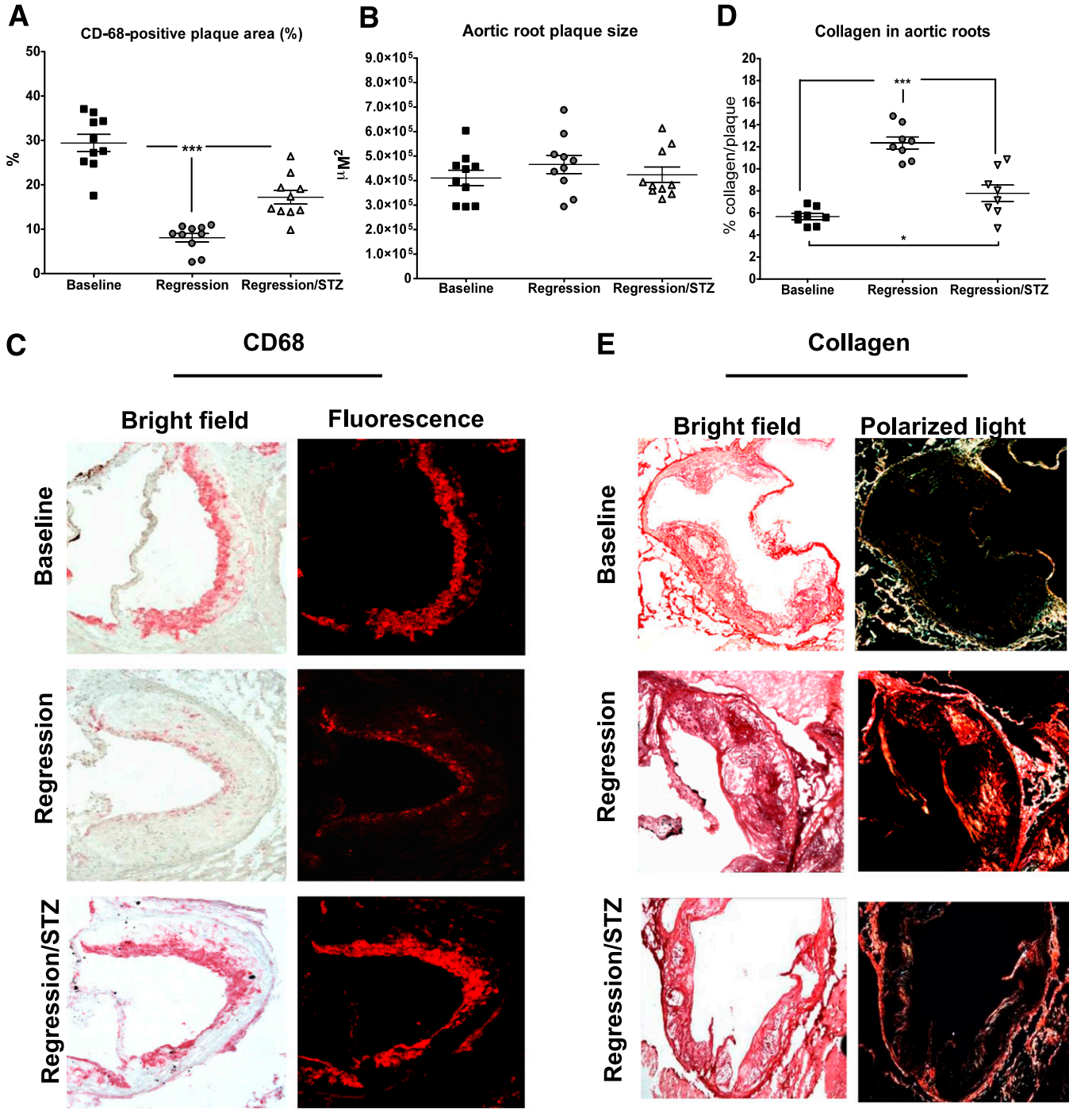

FIG. 2. Diabetic mice have increased CD68+ cell and decreased collagen content compared with nondiabetic mice after plasma lipid reduction. Aortic roots from baseline and the two regression groups were sectioned, fixed, and stained for CD68+ cells. *A*: CD68+ cells as the percentage of plaque area. *B*: Plaque areas quantified by Image Pro Plus software. *C*: Sample pictures of CD68 staining are shown for each group. *D*: Collagen content was determined by picrosirius red staining using both bright field and polarized light microscopy and quantified by Image Pro Plus software. Data are presented as the percentage of lesion area. *E*: Representative sample pictures of collagen staining are shown for each group. Each group contains 8–10 animals. Data (means ± SEM) were analyzed using one-way ANOVA followed by Bonferroni's multiple comparison test. *P* values are shown as **P* < 0.05 and ****P* < 0.001. (A high-quality digital representation of this figure is available in the online issue.)

baseline mice (0.41 ± 0.1 mm^2, Fig. 2*B*). We hypothesized that the composition of extracellular matrix was altered during the regression process. As shown in Fig. 2*D* and *E*, the collagen content was increased by 100% in the regression group and by only 37% in the regression/STZ group compared with the baseline group.

Diabetes also impaired the decrease in plaque lipid content during regression. In the baseline group, 20 and 37% of total plaque area were positive for neutral lipids and free cholesterol, respectively (Fig. 3*A–D*). The neutral lipid area decreased to ~5% of the total plaque area in the regression group, but was twice that in the regression/STZ group (~10%). The free cholesterol area decreased from 37% in the baseline group to 17% in the regression group and to 26% in the regression/STZ group.

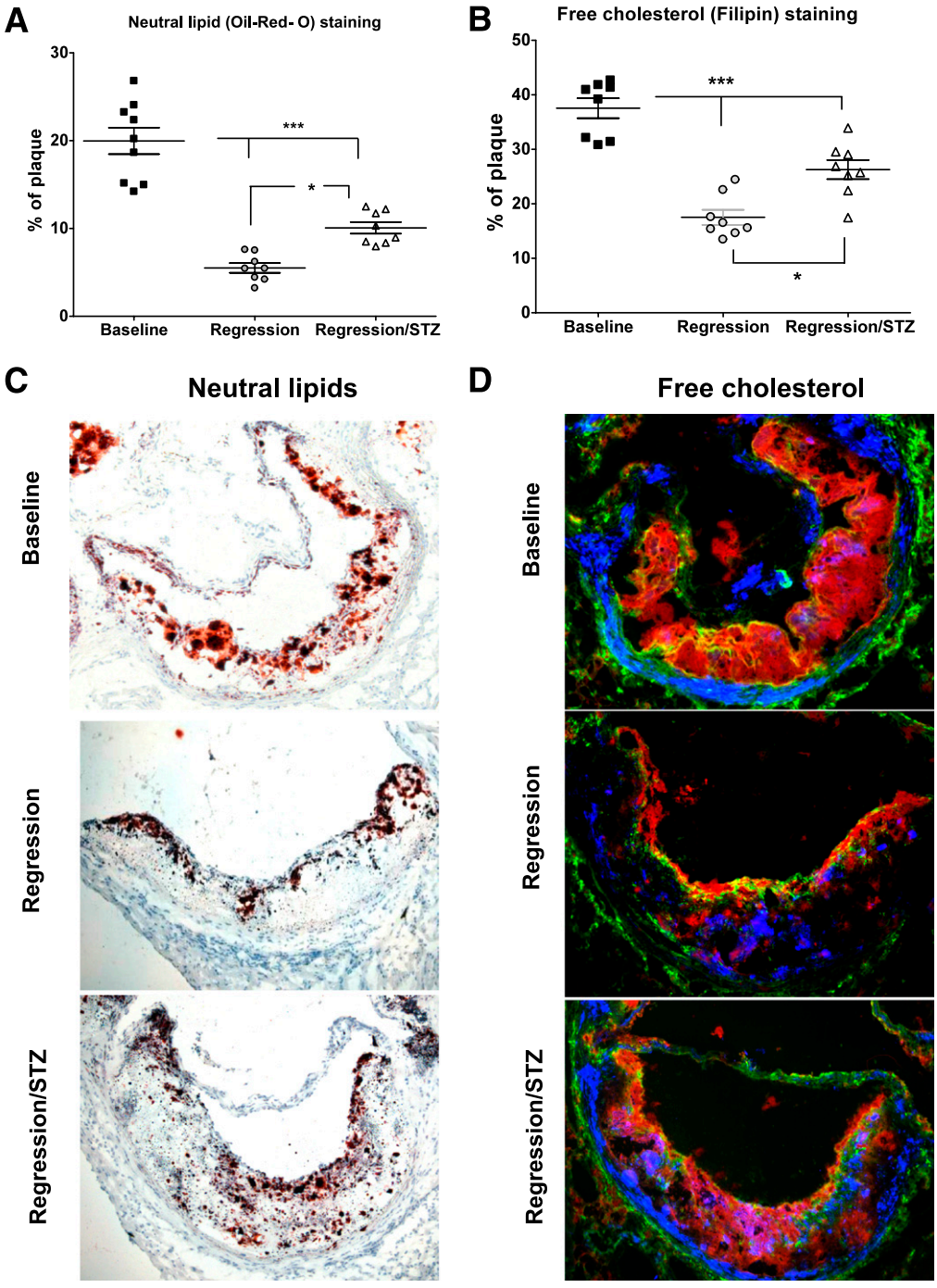

FIG. 3. Effects of diabetes on the lipid content of aortic root sections after plasma lipid reduction. Aortic roots were sectioned, fixed, and stained for neutral lipids (presumably cholesteryl esters) using Oil-Red O or for free cholesterol using filipin. The stained areas were quantified by Image Pro Plus software. Oil-Red O–positive areas (*A*) and free cholesterol (blue staining) (*B*) are quantified and presented as the percentage of total plaque area. Sample pictures of each lipid stain are shown for all experimental groups in *C* and *D*. In addition to filipin staining, immunostaining for CD68 (red) and β-actin (green) are also shown (*D*). Data (means ± SEM) were analyzed using one-way ANOVA followed by Bonferroni's multiple comparison test. $P < 0.05$ values were considered to be significant, $^*P < 0.05$ and $^{***}P < 0.001$. (A high-quality digital representation of this figure is available in the online issue.)

Gene expression in plaque CD68+ cells after the reduction of hyperlipidemia. The expression of genes associated with cell stress and inflammation from plaque laser-captured CD68+ cells tended to be lower in the regression group compared with the baseline group (Table 1). In particular, the regression group had statistically significantly lower expression levels of S100a8, matrix metalloproteinase-2 (MMP-2), inducible nitric-oxide synthase, and IL-1. It is noteworthy that the statistical significance of the regression-associated decreases was lost in the regression/STZ group, with the mean values for these and the other genes in the regression/STZ group either intermediate between those in the other two groups or, in the case of C/EBP homologous protein (CHOP), even higher than that in the baseline group. Markers for alternatively activated M2 macrophages (Arg1, Arg2, Fizz, and IL-10) (21) all showed trends toward an increase in the regression group compared with the baseline group, with the suggestion that diabetes blunted the effects of plasma lipid reduction on these markers.

In a transplant model of regression, the reduction in plaque CD68+ cells was dependent on their emigration through a pathway dependent on CCR7, a chemokine receptor that mediates migration of certain types of leukocytes (6). In the Reversa model, CCR7 expression was also induced by the reduction in hyperlipidemia in the regression group compared with the baseline group (Table 1). In contrast, in the regression/STZ group, CCR7 expression was suppressed compared with the baseline and regression groups, supporting the idea that one explanation for the greater content of plaque CD68+ cells in the regression/STZ versus the regression group (Fig. 2*A* and *C*) is that diabetes impeded their emigration.

TABLE 1
Gene expression analysis of laser-captured plaque CD68+ cells

	Baseline	Regression	Regression/STZ
Stress/inflammation			
CHOP	0.74 ± 0.22	0.14 ± 0.12	1.23 ± 0.64†
S100a8	0.72 ± 0.16	0.12 ± 0.04*	0.35 ± 0.14
MMP-2	2.26 ± 0.40	0.19 ± 0.25*	1.58 ± 0.25
MMP-9	1.38 ± 0.57	0.55 ± 0.41	1.22 ± 0.68
ICAM-1	1.28 ± 0.71	0.78 ± 0.37	1.75 ± 0.56
VCAM-1	1.98 ± 0.07	1.47 ± 0.51	2.34 ± 1.07
iNOS	0.16 ± 0.06	0.02 ± 0.01*	0.05 ± 0.03
IL-1	0.95 ± 0.25	0.08 ± 0.03*	0.34 ± 0.12
Migration			
CCR7	1.19 ± 0.31	8.37 ± 3.43*	0.12 ± 0.05†
M2/anti-inflammatory			
Arg1	10.7 ± 4.32	32.4 ± 18.2	17.0 ± 3.42
Arg2	0.15 ± 0.02	0.41 ± 0.12	0.05 ± 0.05
Fizz	0.21 ± 0.13	0.57 ± 0.18	0.24 ± 0.15
IL-10	0.27 ± 0.10	1.62 ± 0.56	1.24 ± 0.34

Data (mean ± SEM) were analyzed by one-way ANOVA followed by Bonferroni's multiple comparison test. CD68+ cells from aortic roots of Reversa mice were isolated using LCM (each group contained 8–10 animals). mRNA was then isolated and subjected to analyses by RT-PCR. mRNA levels are presented as relative levels normalized to 28S (loading control). ICAM-1, intercellular adhesion molecule-1; iNOS, inducible nitric-oxide synthase; VCAM-1, vascular cell adhesion molecule-1. *$P < 0.05$ was considered to be significant compared with baseline. †$P < 0.05$ was considered to be significant compared with regression.

Hyperglycemia causes changes in macrophage gene expression and in the ability of IL-4 to promote polarization to the M2 phenotypic state. The results above suggested that diabetes may interfere with changes in the inflammatory state and the M2 polarization of macrophages in a regression environment. To simulate the phenomena observed in vivo, we tested in BMDMs whether the hyperglycemic level achieved in the diabetic mice similarly increased inflammatory gene expression or interfered with the potency of IL-4, a commonly used inducer of the M2 state. First, BMDMs in the M0 (unpolarized) state were cultured in normal D-glucose (100 mg/dL) and then switched to a high D-glucose (450 mg/dL) medium or a normal D-glucose medium osmotically matched to the high D-glucose medium by the addition of L-glucose (100 mg/dL D-glucose + 350 mg/dL L-glucose; "normal + L-glucose"). In the high D-glucose medium, there were increased mRNA levels of CHOP, MMP-2, MMP-9, S100a8, inducible nitric oxide synthase, vascular cell adhesion molecule-1, and intercellular adhesion molecule-1 (Table 2), consistent with the results that proatherogenic factors tended to be higher in plaque CD68+ cells from regression/STZ versus regression mice (Table 1). Unlike the LCM data (Table 1), CCR7 mRNA was unaffected by hyperglycemia.

We next examined whether hyperglycemia interfered with IL-4 to polarize macrophages to the alternatively activated M2 state. In high D-glucose (vs. normal D+L-glucose) medium, IL-4–treated BMDMs had decreased expression of two standard markers of the M2 state (Fig. 4*A* and *B*). To extend these data, we also assessed arginase functional activity by measuring urea production, and the pattern was consistent with the mRNA data (Fig. 4*C*).

Because arginase activity is positively associated with collagen production (22,23), we also measured collagen in cultures of IL-4–treated BMDMs under normo- (normal D+L-glucose) and hyperglycemic (high D-glucose) conditions. As shown in Fig. 4*D*, hyperglycemia resulted in an ~70% reduction in collagen.

TABLE 2
Gene expression analysis of BMDMs

	Normal D+L-glucose	High D-glucose
Stress/inflammation		
CHOP	1.00 ± 1.12	1.79 ± 0.15*
S100a8	1.00 ± 0.07	1.86 ± 0.17*
MMP-2	1.00 ± 0.07	1.33 ± 0.08*
MMP-9	1.00 ± 0.11	2.27 ± 0.24*
ICAM-1	1.00 ± 0.02	2.94 ± 0.14*
VCAM-1	1.00 ± 0.14	4.45 ± 0.35*
iNOS	1.00 ± 0.18	2.45 ± 0.17*
Migration		
CCR7	1.00 ± 0.15	1.69 ± 0.42

Data (mean ± SEM) were analyzed using a Student two-tailed *t* test. For each experiment, BMDMs were pooled from two to three Reversa animals at 6–8 weeks of age. BMDMs were maintained in culture medium containing macrophage colony-stimulating factor (10 ng/mL) for 7 days and then treated with medium containing high D-glucose (450 mg/dL) or normal D+L-glucose (100 mg/dL D-glucose + 350 mg/dL L-glucose) for 24 h. RT-PCR was performed as described in RESEARCH DESIGN AND METHODS, and 28S RNA was used as a loading control. The results are from two experiments performed in triplicate. ICAM-1, intercellular adhesion molecule-1; iNOS, inducible nitric-oxide synthase; VCAM-1, vascular cell adhesion molecule-1. *$P < 0.05$ was considered to be significant.

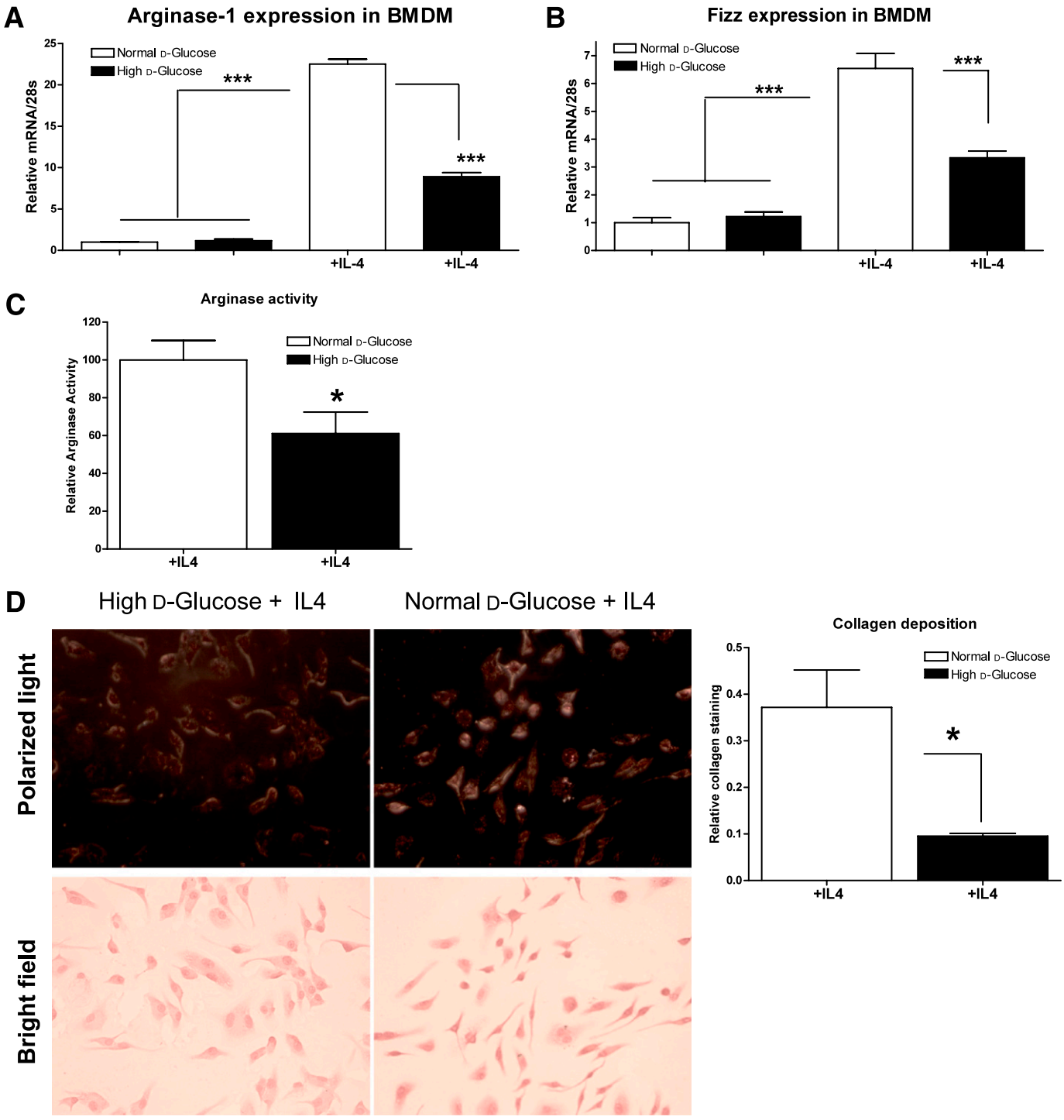

FIG. 4. Hyperglycemia blunts macrophage polarization in vitro by IL-4. For each experiment, BMDMs were pooled from two to three Reversa animals and differentiated into M0 (unactivated) macrophages. The cells were then treated with or without IL-4 (to induce M2 polarization) in normal D+L-glucose (100 mg/dL D-glucose + 350 mg/dL L-glucose) or high D-glucose (450 mg/dL) for 24 h. RT-PCR was performed, and 28S mRNA was used as a normalizing variable. Results shown are for arginase 1 (*A*) and Fizz (*B*). *C*: Arginase functional activity was measured by urea production according to the manufacturer's protocol (QuantiChrom; BioAssay Systems, Hayward, CA). *D*: Collagen content of cultured BMDM treated with IL-4 (10 ng/mL) for 48 h in normal or high glucose was determined by picosirius red staining and quantified using polarized light microscopy. Stained areas were quantified by Image Pro Plus software. Data (means ± SEM) were analyzed using one-way ANOVA followed by Bonferroni's multiple comparison test (*A* and *B*) or Student two-tailed *t* test (*C* and *D*). *$P < 0.05$ and ***$P < 0.001$ values were considered to be significant. (A high-quality color representation of this figure is available in the online issue.)

Hyperglycemia increases oxidative stress and alters morphology of BMDM. Oxidative stress has been shown to increase macrophage spreading/adhesion and to reduce cell migration (24,25). These effects led to increased arterial intima macrophage retention in an in vivo model (25). Because hyperglycemia (26,27) and hyperlipidemia (28) increase cellular oxidative stress (29,30), we examined levels of reactive oxygen species (ROS) in the plaques in the three groups. As shown in Fig. 5*A*, there was a significant reduction in ROS levels in the regression group

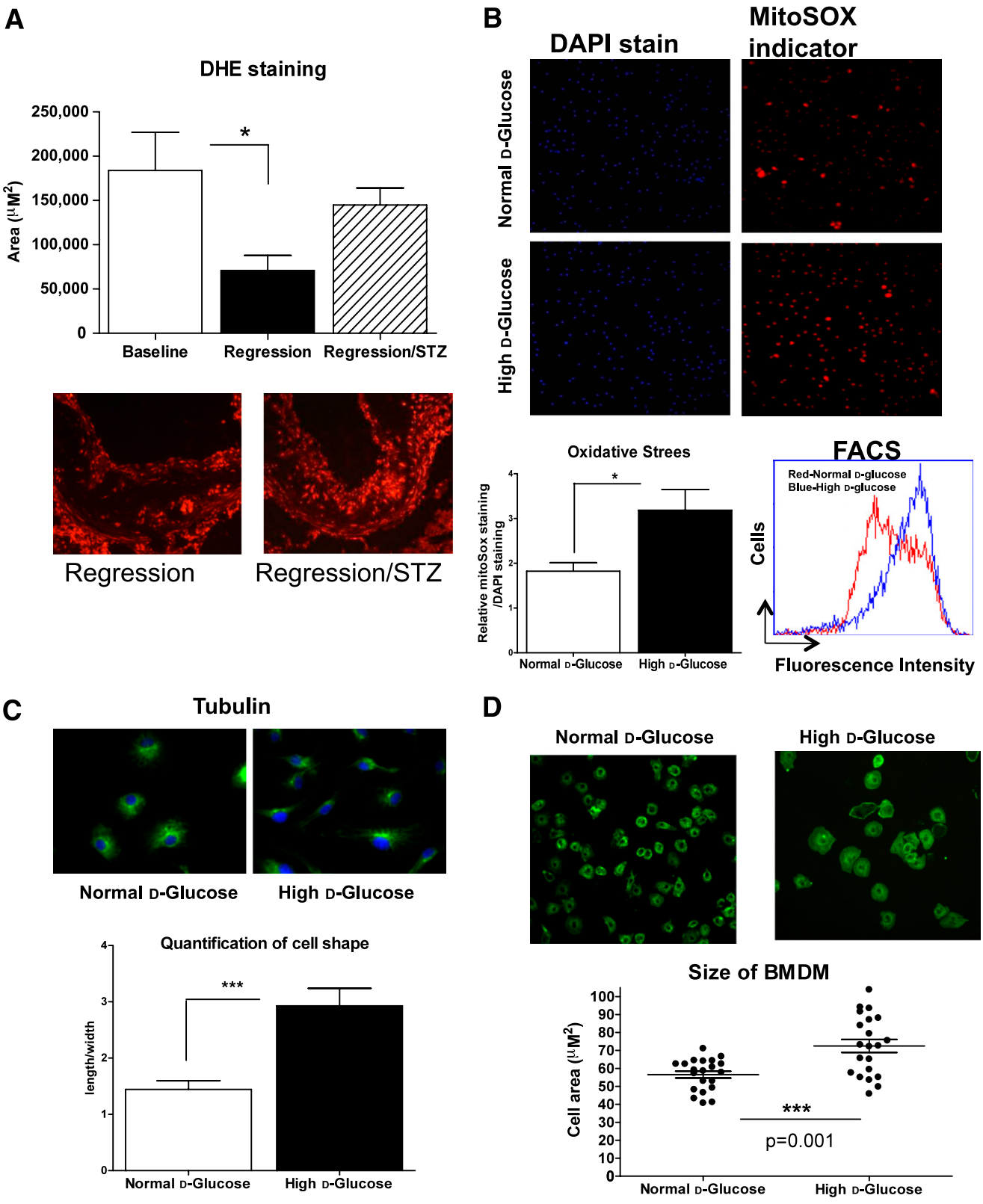

FIG. 5. Hyperglycemia increased oxidative stress in vivo and in vitro, and altered macrophage morphology and cell spreading in vitro. *A*: Frozen aortic root sections from baseline, regression, and STZ/regression mice were stained with dihydroethidium to assess oxidative stress. The area stained was quantified by Image Pro Plus software, and representative images from the regression and regression/STZ groups are shown. *B*: BMDMs were incubated with DMEM containing normal D+L-glucose (100 mg/dL D-glucose + 350 mg/dL L-glucose) or high D-glucose (450 mg/dL) for 24 h. Cellular oxidative stress was determined by staining suspended cells with MitoSOX (Molecular Probes). The cells were then subjected to fluorescence-activated cell sorter analysis (red = normal D-glucose and blue = high D-glucose) or replated on chamber slides and the staining quantified using Image Pro Plus. *C*: BMDMs were also stained with tubulin, and the length and width were measured with Image Pro Plus software. *D*: For spreading experiments, cells were treated as above and replated on collagen-coated slides for 2 h and then stained with FITC-phalloidin following the manufacturer's protocol (Invitrogen). Cell areas were determined using Image Pro Plus. Data (means ± SEM) were analyzed using one-way ANOVA followed by Bonferroni's multiple comparison test (*A*) or Student two-tailed *t* test (*B–D*). *$P < 0.05$ and ***$P < 0.001$ values were considered to be significant. (A high-quality digital representation of this figure is available in the online issue.)

compared with baseline that was not observed in the regression/STZ group.

Hyperglycemia also increased ROS content in BMDMs, as determined by staining for H_2O_2 (Fig. 5*B*). Fluorescence-activated cell sorter analysis also showed that BMDMs incubated in high D-glucose had a 44% increase (vs. incubation in normal D+L-glucose) in staining for H_2O_2 as determined by mean fluorescence (Fig. 5*B*).

Hyperglycemia also caused striking morphologic changes in vitro. As shown in Fig. 5*C* and *D*, BMDMs incubated in high D-glucose were significantly larger, more spread, and spindle-shaped than cells grown in normal D+L-glucose. The differences in cell morphology were quantified by measuring the length versus width, as well as the cell area.

DISCUSSION

The development of atherosclerosis that culminates in a clinical event is neither continuous nor unidirectional. Especially within the setting of diabetes, arterial pathology in humans likely fluctuates with changes in risk factors, such as dyslipidemia and hyperglycemia. It is currently recommended that patients with diabetes be treated aggressively for both of these risk factors to retard the progression of coronary artery disease and, ideally, to promote plaque regression. To simulate therapeutic LDL lowering in a model of atherosclerosis, we have used Reversa mice. By conditionally inactivating the *Mttp* gene, hyperlipidemia can be dramatically reduced at any time in these mice (11). In the current study, we have allowed advanced plaques to develop in Reversa mice before inactivating the *Mttp* gene. Concomitant with the reduction of hyperlipidemia, half of the mice were treated with STZ to produce diabetes to study whether plaque regression, as judged by the content of CD68+ cells, would be impaired. After the reduction in hyperlipidemia, the major effects of diabetes on plaques were the following: *1*) impaired decrease in the content of CD68+ cells and free and esterified cholesterol; *2*) increased expression in CD68+ cells of genes considered to be detrimental in atherosclerosis and decreased enrichment of those associated with the alternatively activated M2 state of macrophages; *3*) reduced accumulation of collagen; and *4*) increased oxidant stress. Furthermore, studies in vitro, in which BMDMs were incubated in normoglycemic or hyperglycemic conditions, recapitulated many of the findings in vivo.

We have previously observed that plaque regression involved the emigration of CD68+ cells (6,31), which was dependent on CCR7, a chemokine receptor that promotes the migration of certain classes of leukocytes (32,33). In this study, plaques from the regression/STZ group contained more CD68+ cells than the regression group, consistent with decreased expression of CCR7 in vivo (Table 1), although hyperglycemia did not significantly affect CCR7 expression in vitro. The increased cell spreading in vitro (Fig. 5*D*) was also consistent with a decreased migratory ability of cells in a hyperglycemic environment.

The effects of hyperglycemia on cell morphology may also be related to migration, given the recent findings that macrophages incubated in high glucose medium had increased activity of the ρ-associated coiled–coil protein kinase, a major participant in cytoskeletal reorganization (34). Decreased CD68+ cell emigration in the regression/STZ plaques would also be compatible with the slower wound healing in patients with diabetes, attributed in part to impaired chemotaxis of skin fibroblasts (35,36). Nonetheless, we cannot rule out the possibility that diabetes also contributed to limiting the decrease in plaque CD68+ cell content after lipid lowering by increasing the influx of circulating monocytes into the plaque.

As noted above, despite equivalent plasma lipid lowering in both regression groups, the plaque content of cholesterol and cholesteryl ester was greater in the regression/STZ group. This was likely related to there being more CD68+ foam cells in these plaques, although there was also the suggestion that there was more extracellular lipid (Fig. 3). Another contributing factor may have been reduced levels of ATP-binding cassette transporters in the macrophages of the diabetic mice (37).

Plaques of hyperlipidemic diabetic mice have been reported to have increased inflammatory gene expression (38), but whether this was due to effects on a per cell basis or greater numbers of inflammatory macrophages could not be distinguished. By using LCM, the present data demonstrate that even in the absence of hyperlipidemia, diabetes impairs the resolution of the inflammatory state in individual cells, a characteristic shared with macrophages in progressing plaques (39). Macrophages in the inflammatory state are often referred to as being M1, as opposed to those with anti-inflammatory properties (40), termed "M2," although acceptance of this simple classification is controversial (41). Nonetheless, macrophages in human and mouse atherosclerotic plaques display both M1 and M2 markers (9,10).

In the context of plaque regression, there would be considerable advantage to the polarization of CD68+ cells to the M2 state, because they are known to promote the remodeling of damaged tissue (42). In addition to the impairment of the reduction of plaque CD68+ content, another deleterious effect of diabetes may be the interference with favorable changes in macrophage phenotype after plasma lipid reduction, based on the data in Table 1 as reviewed in RESULTS.

The hyperglycemia, and not the insulin deficiency of STZ-diabetes, exerted the strong independent and negative effects on the phenotypic state of plaque CD68+ cells, as supported by the studies in vitro. Gene expression changes in the regression/STZ group were paralleled in BMDMs incubated in medium containing the same glucose concentration as measured in the diabetic mice. In addition, the potency of the standard M2 inducer, IL-4, was attenuated by incubating the cells in hyperglycemic medium. These results could not be explained by changes in osmolarity and are unlikely caused by toxicity of hyperglycemia on BMDM (43).

It was also remarkable that, in the regression/STZ group, there was less plaque collagen accumulation than in the normoglycemic mice. This may have also been a reflection of the effects of diabetes on macrophage polarization, because M2 macrophages are known to promote collagen synthesis (44). Other possible explanations include the greater expression of matrix-degrading enzymes MMP-2 and -9 that we found in vivo, as well as effects on plaque smooth muscle cells, a major source of collagen in the arterial wall, although the number of such cells did not vary between the regression and regression/STZ groups (data not shown). Consistent with the data in vivo, BMDMs incubated in hyperglycemic medium had reduced expression of M2 markers and collagen production.

As reviewed by Hirsch and Brownlee (45) and Brownlee (46), an overarching feature of diabetic hyperglycemia

responsible for many manifestations of glucotoxicity is the promotion of cellular oxidative stress. The effects of oxidative stress include the release of proinflammatory cytokines, such as IL-1 (47), from macrophages. This is consistent with the present data under hyperglycemic conditions in vivo and in vitro. In particular, the incubation of BMDM in the high glucose medium increased ROS. Even more significantly, the plaques in the regression/STZ group demonstrated increased oxidant stress despite the reduction of hyperlipidemia, another known ROS-elevating factor. Given that oxidant stress in the plaques of regression/STZ mice approached the level in the plaques of baseline mice (Fig. 5), the data suggest that hyperglycemia is an inducer of ROS comparable in potency to hyperlipidemia.

Current treatment guidelines emphasize that optimal care of the diabetic patient includes aggressive management of their dyslipidemia. An animal model to clinically simulate this scenario has been elusive, but the development of the Reversa mouse has now allowed us to conveniently test the effects of hyperglycemia on the process of plaque regression after a dramatic reduction of plasma LDL. In general, many of the benefits on plaque composition (fewer macrophages, more collagen) and CD68+ cell phenotype (less inflammation, more M2-like characteristics) after lipid reduction were attenuated in the diabetic mice. Although there are many differences between STZ-induced diabetic mice and patients with diabetes (typically type 2 diabetes mellitus), the present data are consistent with clinical studies showing that the absolute risk of myocardial infarction remains higher in patients with diabetes even after statin therapy (48). The molecular exploration of mouse models of atherosclerosis regression may ultimately explain why this is the case.

ACKNOWLEDGMENTS

These studies were supported by National Institutes of Health grants U01-HL-0879450 and HL-084312.

No potential conflicts of interest relevant to this article were reported.

S.P. collected and analyzed data and drafted the article; L.G. provided experimental assistance; L.-S.H. collected and analyzed data; M.S. and E.D. provided experimental support in the area of BMDMs; and I.J.G. and E.A.F. contributed to the design of the experiments and the data analysis and interpretation and revised the article.

The authors thank Dr. Jonathan E. Feig from New York University for helpful discussions; Dr. Konstantinos Drosatos and Dr. Prabhakara Nagareddy from Columbia University for provision of mouse plasma samples; Dr. Shuiqing Yu and Sunny Haft from Columbia for technical assistance; and Dr. Masanoru Aikawa from Harvard Medical School for advice on the collagen detection by polarizing light microscopy.

REFERENCES

1. Haffner SM, Lehto S, Rönnemaa T, Pyörälä K, Laakso M. Mortality from coronary heart disease in subjects with type 2 diabetes and in nondiabetic subjects with and without prior myocardial infarction. N Engl J Med 1998;339:229–234
2. Karlson BW, Herlitz J, Hjalmarson A. Prognosis of acute myocardial infarction in diabetic and non-diabetic patients. Diabet Med 1993;10:449–454
3. Burke AP, Kolodgie FD, Zieske A, et al. Morphologic findings of coronary atherosclerotic plaques in diabetics: a postmortem study. Arterioscler Thromb Vasc Biol 2004;24:1266–1271
4. Timmins JM, Lee J-Y, Boudyguina E, et al. Targeted inactivation of hepatic Abca1 causes profound hypoalphalipoproteinemia and kidney hypercatabolism of apoA-I. J Clin Invest 2005;115:1333–1342
5. Ross R. Atherosclerosis is an inflammatory disease. Am Heart J 1999;138:S419–S420
6. Trogan E, Feig JE, Dogan S, et al. Gene expression changes in foam cells and the role of chemokine receptor CCR7 during atherosclerosis regression in ApoE-deficient mice. Proc Natl Acad Sci U S A 2006;103:3781–3786
7. Martinez FO, Sica A, Mantovani A, Locati M. Macrophage activation and polarization. Front Biosci 2008;13:453–461
8. Gordon S. Alternative activation of macrophages. Nat Rev Immunol 2003;3:23–35
9. Bouhlel MA, Derudas B, Rigamonti E, et al. PPARgamma activation primes human monocytes into alternative M2 macrophages with anti-inflammatory properties. Cell Metab 2007;6:137–143
10. Khallou-Laschet J, Varthaman A, Fornasa G, et al. Macrophage plasticity in experimental atherosclerosis. PLoS ONE 2010;5:e8852
11. Lieu HD, Withycombe SK, Walker Q, et al. Eliminating atherogenesis in mice by switching off hepatic lipoprotein secretion. Circulation 2003;107:1315–1321
12. Like AA, Rossini AA. Streptozotocin-induced pancreatic insulitis: new model of diabetes mellitus. Science 1976;193:415–417
13. Zhang X, Goncalves R, Mosser DM. The isolation and characterization of murine macrophages. Curr Protoc Immunol 2008;Chapter 14:Unit 14.1
14. Choudhury RP, Rong JX, Trogan E, et al. High-density lipoproteins retard the progression of atherosclerosis and favorably remodel lesions without suppressing indices of inflammation or oxidation. Arterioscler Thromb Vasc Biol 2004;24:1904–1909
15. Junqueira LC, Bignolas G, Brentani RR. Picrosirius staining plus polarization microscopy, a specific method for collagen detection in tissue sections. Histochem J 1979;11:447–455
16. Rong JX, Shapiro M, Trogan E, Fisher EA. Transdifferentiation of mouse aortic smooth muscle cells to a macrophage-like state after cholesterol loading. Proc Natl Acad Sci U S A 2003;100:13531–13536
17. Kellner-Weibel G, Geng YJ, Rothblat GH. Cytotoxic cholesterol is generated by the hydrolysis of cytoplasmic cholesteryl ester and transported to the plasma membrane. Atherosclerosis 1999;146:309–319
18. Sorescu D, Weiss D, Lassègue B, et al. Superoxide production and expression of nox family proteins in human atherosclerosis. Circulation 2002;105:1429–1435
19. Nunnari JJ, Zand T, Joris I, Majno G. Quantitation of oil red O staining of the aorta in hypercholesterolemic rats. Exp Mol Pathol 1989;51:1–8
20. Feng B, Zhang D, Kuriakose G, Devlin CM, Kockx M, Tabas I. Niemann-Pick C heterozygosity confers resistance to lesional necrosis and macrophage apoptosis in murine atherosclerosis. Proc Natl Acad Sci U S A 2003;100:10423–10428
21. Edwards JP, Zhang X, Frauwirth KA, Mosser DM. Biochemical and functional characterization of three activated macrophage populations. J Leukoc Biol 2006;80:1298–1307
22. Durante W, Liao L, Reyna SV, Peyton KJ, Schafer AI. Transforming growth factor-beta(1) stimulates L-arginine transport and metabolism in vascular smooth muscle cells: role in polyamine and collagen synthesis. Circulation 2001;103:1121–1127
23. Schnoor M, Cullen P, Lorkowski J, et al. Production of type VI collagen by human macrophages: a new dimension in macrophage functional heterogeneity. J Immunol 2008;180:5707–5719
24. Ryu JW, Hong KH, Maeng JH, et al. Overexpression of uncoupling protein 2 in THP1 monocytes inhibits beta2 integrin-mediated firm adhesion and transendothelial migration. Arterioscler Thromb Vasc Biol 2004;24:864–870
25. Park YM, Febbraio M, Silverstein RL. CD36 modulates migration of mouse and human macrophages in response to oxidized LDL and may contribute to macrophage trapping in the arterial intima. J Clin Invest 2009;119:136–145
26. Dasu MR, Devaraj S, Jialal I. High glucose induces IL-1beta expression in human monocytes: mechanistic insights. Am J Physiol Endocrinol Metab 2007;293:E337–E346
27. Venugopal SK, Devaraj S, Yang T, Jialal I. Alpha-tocopherol decreases superoxide anion release in human monocytes under hyperglycemic conditions via inhibition of protein kinase C-alpha. Diabetes 2002;51:3049–3054
28. Tripathy D, Mohanty P, Dhindsa S, et al. Elevation of free fatty acids induces inflammation and impairs vascular reactivity in healthy subjects. Diabetes 2003;52:2882–2887
29. Witztum JL. The oxidation hypothesis of atherosclerosis. Lancet 1994;344:793–795
30. Witztum JL, Steinberg D. Role of oxidized low density lipoprotein in atherogenesis. J Clin Invest 1991;88:1785–1792
31. Llodrá J, Angeli V, Liu J, Trogan E, Fisher EA, Randolph GJ. Emigration of monocyte-derived cells from atherosclerotic lesions characterizes

regressive, but not progressive, plaques. Proc Natl Acad Sci U S A 2004;101:11779–11784
32. Förster R, Schubel A, Breitfeld D, et al. CCR7 coordinates the primary immune response by establishing functional microenvironments in secondary lymphoid organs. Cell 1999;99:23–33
33. Menning A, Höpken UE, Siegmund K, Lipp M, Hamann A, Huehn J. Distinctive role of CCR7 in migration and functional activity of naive- and effector/memory-like Treg subsets. Eur J Immunol 2007;37:1575–1583
34. Cheng C-I, Cheng S-M, Li Y, Zhou Q, Liao JK. Abstract 5571: Induction of macrophage activation and foam cell formation by high glucose is mediated by Rho-associated coiled-coil forming kinase. Circulation 2009;120:S1119-a
35. Ramsey SD, Newton K, Blough D, et al. Incidence, outcomes, and cost of foot ulcers in patients with diabetes. Diabetes Care 1999;22:382–387
36. Khanna S, Biswas S, Shang Y, et al. Macrophage dysfunction impairs resolution of inflammation in the wounds of diabetic mice. PLoS ONE 2010;5:e9539
37. Tang C, Oram JF. The cell cholesterol exporter ABCA1 as a protector from cardiovascular disease and diabetes. Biochim Biophys Acta 2009;1791:563–572. Epub 2009 Apr 1
38. Johansson F, Kramer F, Barnhart S, et al. Type 1 diabetes promotes disruption of advanced atherosclerotic lesions in LDL receptor-deficient mice. Proc Natl Acad Sci U S A 2008;105:2082–2087
39. Tabas I. Macrophage death and defective inflammation resolution in atherosclerosis. Nat Rev Immunol 2010;10:36–46. Epub 2009 Dec 4
40. Mosser DM, Edwards JP. Exploring the full spectrum of macrophage activation. Nat Rev Immunol 2008;8:958–969
41. Geissmann F, Gordon S, Hume DA, Mowat AM, Randolph GJ. Unravelling mononuclear phagocyte heterogeneity. Nat Rev Immunol 2010;10:453–460
42. Deonarine K, Panelli MC, Stashower ME, et al. Gene expression profiling of cutaneous wound healing. J Transl Med 2007;5:11
43. Vats D, Mukundan L, Odegaard JI, et al. Oxidative metabolism and PGC-1beta attenuate macrophage-mediated inflammation. Cell Metab 2006;4:13–24
44. Sandler NG, Mentink-Kane MM, Cheever AW, Wynn TA. Global gene expression profiles during acute pathogen-induced pulmonary inflammation reveal divergent roles for Th1 and Th2 responses in tissue repair. J Immunol 2003;171:3655–3667
45. Hirsch IB, Brownlee M. Should minimal blood glucose variability become the gold standard of glycemic control? J Diabetes Complications 2005;19:178–181
46. Brownlee M. Biochemistry and molecular cell biology of diabetic complications. Nature 2001;414:813–820
47. Fuhrman B, Oiknine J, Aviram M. Iron induces lipid peroxidation in cultured macrophages, increases their ability to oxidatively modify LDL, and affects their secretory properties. Atherosclerosis 1994;111:65–78
48. Deedwania P, Barter P, Carmena R, et al.; Treating to New Targets Investigators. Reduction of low-density lipoprotein cholesterol in patients with coronary heart disease and metabolic syndrome: analysis of the Treating to New Targets study. Lancet 2006;368:919–928